Pseudo-Ginsenoside Rh2 induces A549 cells apoptosis via the Ras/Raf/ERK/p53 pathway

YUCHEN WANG[1,2*], HUALI XU[1*], ZEYUAN LU[1], XIAOFENG YU[1], CHEN LV[1], YUAN TIAN[1] and DAYUN SUI[1]

[1]Department of Pharmacology, School of Pharmaceutical Sciences, Jilin University, Changchun, Jilin 130021; [2]School of Pharmaceutical Sciences, Changchun University of Chinese Medicine, Changchun, Jilin 130117, P.R. China

Received November 6, 2017; Accepted February 22, 2018

DOI: 10.3892/etm.2018.6067

Abstract. Ginsenoside Rh2, a major effective constituent of ginseng, has been suggested to have a pro-apoptotic effect in a variety of cancer cells. Pseudo-Ginsenside-Rh2 (pseudo-G-Rh2) is a novel derivative of ginsenoside Rh2. The aim of the present study was to evaluate the effect of pseudo-G-Rh2 on the apoptosis of lung adenocarcinoma A549 cells. The cytotoxicity of pseudo-G-Rh2 on A549 cells was evaluated using an MTT assay. Apoptosis was detected using DAPI staining and flow cytometry. The expression of apoptosis associated proteins was identified by western blot analysis. The results demonstrated that pseudo-G-Rh2 inhibits the proliferation of A549 cells in a dose-dependent manner. DAPI staining revealed topical morphological changes in apoptotic bodies following pseudo-G-Rh2 treatment. Flow cytometric analysis revealed that the percentage of Annexin V-fluorescein isothiocyanate-positive cells, which are apoptotic, increased with pseudo-G-Rh2 treatment in a dose-dependent manner. Furthermore, treatment with pseudo-G-Rh2 increased the level of reactive oxygen species in A549 cells as well as the activation of caspase-9, caspase-3 and poly ADP-ribose polymerase. Pseudo-G-Rh2 treatment was observed to induce mitochondrial membrane potential loss. Furthermore, the results of western blotting revealed that B-cell lymphoma 2 (Bcl-2) expression was significantly decreased while Bcl-2-associated X protein expression was significantly upregulated in A549 cells with pseudo-G-Rh2 treatment. Pseudo-G-Rh2-induced apoptosis was accompanied by sustained phosphorylation of Ras, Raf, extracellular signal-regulated kinase (ERK) and p53. In conclusion, the results of the present study suggest that pseudo-G-Rh2 induces mitochondrial apoptosis in A549 cells and is responsible for excessive activation of the Ras/Raf/ERK/p53 pathway.

Correspondence to: Dr Dayun Sui, Department of Pharmacology, School of Pharmaceutical Sciences, Jilin University, 1266 Fujin Road, Changchun, Jilin 130021, P.R. China
E-mail: suidy@jlu.edu.cn

*Contributed equally

Key words: pseudo-ginsenoside-Rh2, apoptosis, A549, caspase

Introduction

For the past 30 years, lung cancer has been the primary cause of cancer-associated mortality in China (1). Specifically, >80% of all lung cancer cases are non-small cell lung cancer (NSCLC), with adenocarcinoma being the most prevalent NSCLC subtype (2). Despite increased understanding of lung adenocarcinoma, the 5-year survival rate remains <17% (3-5). It is therefore of great importance to develop novel therapeutic targets and effective treatments to improve the prognoses of patients with adenocarcinoma.

The extracellular signal-regulated kinase (ERK) family is typically considered to been associated with the proliferation, differentiation and migration of cells (6). However, a number of studies have reported that activation of the Ras/Raf/ERK pathway may induce apoptosis, autophagy and senescence in tumor cells under certain circumstances (7,8). Several commonly used chemotherapeutic agents, including piperlongumine (9), paclitaxel (10) and Wentilactone A (11), activate the Ras/Raf/ERK pathway to extert an anti-proliferative effect.

Ginseng, the root of *Panax ginseng* C.A. Meyer (Araliaceae), has been used as a traditional herbal medicine in China for centuries (12). Ginseng possesses a number of pharmacological activities, including immunomodulatory, anti-mutagenic and anti-aging effects (13). Ginsenoside Rh2 (G-Rh2) is one of the primary effective constituents of ginseng and has been reported to induce apoptosis in human lung adenocarcinoma A549 cells and human breast cancer MCF-7 cells (14,15).

In a previous study, a number of dammarane-type derivatives were prepared and their activities were investigated (16). Qian *et al* (17) at the College of Chemistry of Jilin University designed a novel dammarane-type derivative, namely β-D-Glucopyranoside,(3b,12b,20E)-12,25-dihydroxy dammar-20 (22)-en-3-yl, pseudo-G-Rh2, which possesses a different side chain at C-17 compared with G-Rh. In a previous study by our group, pseudo-G-Rh2 was reported to induce apoptosis in human gastric cancer SGC-7901 cells *in vitro* (18). However, whether pseudo-G-Rh2 induces apoptosis in lung adenocarcinoma A549 cells remains unclear. The aim of the

present study therefore was to elucidate the antitumor effects of pseudo-G-Rh2 in lung adenocarcinoma cells.

Materials and methods

Chemicals. Pseudo-G-Rh2 (Fig. 1) was provided by Professor Chen (College of Chemistry, Jilin University, Changchun, China). The purity of pseudo-G-Rh2 used in experiments was >95% as assessed by high-performance liquid chromatography using Agilent 1100 with a Zoebax Extent C18 column (250x4.6 mm, 5 μm) (both, Agilent Technologies, Inc., Santa Clara, CA, USA) at 25˚C. Methanol and water (90:10) was used as the mobile phase, the flow rate was 1.2 ml/min and the sample quantity was 10 μl). Antibodies against procaspase-3 (cat. no. 19677-1-AP), procaspase-9 (cat. no. 66169-1-Ig) and β-actin (cat. no. 20536-1-AP) were purchased from Wuhan Sanying Biotechnology (Wuhan, China). Antibodies against PARP (cat. no. 9542), Bcl-2 (cat. no. 2876), Bax (cat. no. 2772), Ras (cat. no. 3965), phosphorylated (p)-Raf (cat. no. 9427), Raf (cat. no. 9422), p53 (cat. no. 9282), ERK (cat. no. 4695), c-Jun N-terminal kinase (JNK) (cat. no. 9258), p38 (cat. no. 8690), p-ERK (cat. no. 4370), p-JNK (cat. no. 4668) and p-p38 (cat. no. 4511) were purchased from Cell Signaling Technology, Inc. (Danvers, MA, USA). The BCA protein assay reagent kit, DAPI staining kit, reactive oxygen species (ROS) assay kit (cat. no. S0033) and Rhodamine 123 were purchased from Beyotime Institute of Biotechnology (Jiangsu, China). An Annexin V-fluorescein isothiocyanate (FITC) apoptosis detection kit was obtained from Tianjin Sungene Biotech Co., Ltd. (Tianjin, China). MTT and all other reagents were purchased from Sigma-Aldrich (Merck KGaA, Darmstadt, Germany).

Cell culture and treatment. Lung adenocarcinoma A549 cells were obtained from the Shanghai Institute of Cell Biology, Chinese Academic of Sciences (Shanghai, China). A549 cells were cultured in RPMI-1640 medium (Gibco; Thermo Fisher Scientific, Inc., Waltham, MA, USA) supplemented with 10% fetal bovine serum (Zhejiang Tianhang Biotechnology Co., Ltd., Huzhou, China) under standard culture conditions (37˚C in an atmosphere containing 5% CO_2). Culture medium was replaced every 3 days with fresh complete medium and maintained in log phase growth. Pseudo-G-Rh2 was dissolved in dimethyl sulfoxide (DMSO) at room temperature and 104 μM was the maximum solubility. Then Pseudo-G-Rh2 was added to the culture media at the final concentrations. The final concentration of DMSO was <0.1%. Cells were treated with different concentrations of Pseudo-G-Rh2 (40, 56, 72, 88 or 104 μM) for 24, 48 and 72 h at 37˚C, prior to an MTT assay. The cells were administered with 24, 48 or 96 μM Pseudo-G-Rh2 for 24 h at 37˚C prior to DAPI staining, flow cytometry and western blot analysis.

MTT assay. Cell viability was assessed using an MTT assay as previously described (19). Briefly, A549 cells were seeded into 96-well plates (5x10^4/ml) following treatment with 40, 56, 72, 88 or 104 μM pseudo-G-Rh2. Cells were incubated for 20 h at 37˚C. A total of 10 μl of MTT solution (5 mg/ml in PBS) was added to each well and plates were incubated for a further 4 h at 37˚C. A total of 100 μl DMSO was added to each well and plates were agitated for 10 min. Absorbance was measured at 570 nm using a microplate reader (SpectraMax 340PC384; Molecular Devices LLC, Sunnyvale, CA, USA). Cell viability was calculated as a fraction of the untreated cells. The half-maximal inhibitory concentration (IC50) was calculated using GraphPad Prism v5 (GraphPad Software, Inc., La Jolla, CA, USA).

DAPI staining. DAPI staining was performed as previously described (20). Briefly, A549 cells were seeded on 6-well plates (9x10^4/ml) and treated with 24, 48 and 96 μM pseudo-G-Rh2 at 37˚C for 24 h. Cells were collected and washed twice with PBS, permeabilized with 0.1% Triton X-100 and stained with 2 μg/ml DAPI for 10 min at room temperature. Cells were subsequently observed using a fluorescence microscope (magnification, x100; Nikon TE-2000U; Nikon Corporation, Tokyo, Japan).

Annexin V-FITC/propidium iodide (PI) assay. To assess pseudo-G-Rh2-induced apoptosis in A549 cells, Annexin V-FITC/PI staining and flow cytometry were performed as previously described with an (19). Briefly, following pseudo-G-Rh2 treatment, A549 cells were collected, washed twice with PBS and resuspended in 300 μl of binding buffer containing PI and Annexin V-FITC. The samples were incubated for 15 min at room temperature in dark and subsequently detected by flow cytometry and CellQuest™ Pro (version 6.0) software (BD Biosciences, Franklin Lakes, NJ, USA).

Caspase activity assay. The activities of caspase-3 and caspase-9 were measured using a caspase 3 Activity Assay kit (cat. no. C1115) and caspase 9 Activity Assay kit (cat. no. C1157) according to the manufacturer's protocol (both Beyotime Institute of Biotechnology). Briefly, cell lysates were incubated in a radioimmunoprecipitation lysis buffer (cat. no. P0013B; Beyotime Institute of Biotechnology) for 15 min on ice and centrifuged at 18,000 x g for 10 min at 4˚C. Supernatants were collected and total protein was quantified using the Bradford method. Protein lysates was mixed with reaction buffer (Ac-DEVD-pNA for caspase-3, Ac-LEHD-pNA for caspase-9) and incubated at 37˚C for 2 h in the dark. Cell absorbance was subsequently measured at 405 nm using a microplate reader. Results were reported as the percentage activity change compared with the control.

Mitochondrial membrane potential ($\Delta\Psi m$). The $\Delta\Psi m$ was measured using the cationic dye Rhodamine 123 (cat. no. C2007; Beyotime Institute of Biotechnology) as previously described (21). Briefly, A549 cells were treated with 24, 48 and 96 μM pseudo-G-Rh2 for 24 h and incubated with Rhodamine 123 at 37˚C for 30 min. Fluorescence intensities were analyzed by flow cytometry and CellQuest™ Pro software as above.

Measurement of ROS. ROS levels were assessed using the nonfluorescent probe 2',7'-dichlorofluorescein diacetate (DCFH-DA; Beyotime Institute of Biotechnology) as previously described (22). DCFH-DA permeates into cells and is deacetylated by nonspecific esterase in the cell to form 2',7'-dichlorofluorescein, which is nonfluorescent. The cellular oxidizing agent oxidize DCFH to dichlorofluorescein, which

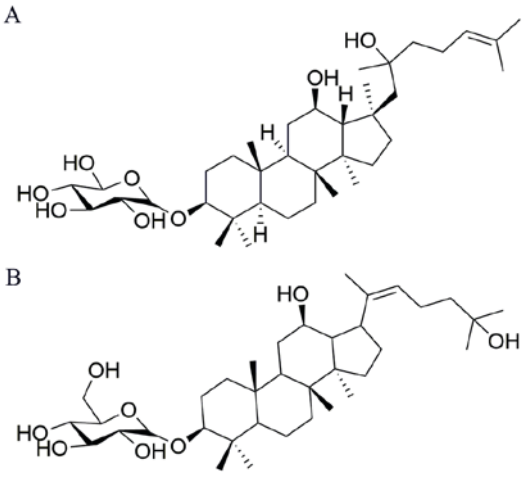

Figure 1. The chemical structures of (A) G-Rh2 and (B) pseudo-G-Rh2. G, ginsenoside.

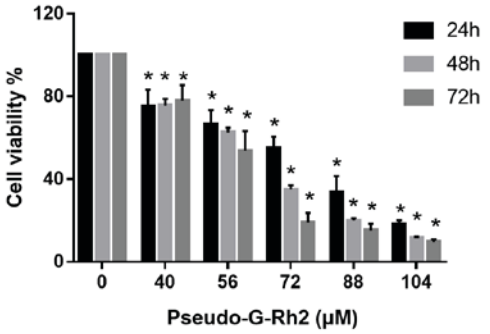

Figure 2. Effects of pseudo-G-Rh2 on the viability of A549 cells. An MTT assay was performed to assess cell viability following treatment with 0, 40, 56, 72 and 88 μM pseudo-G-Rh2 for 24, 48 or 72 h. *P<0.05 vs. control. G, ginsenoside.

is a highly fluorescent compound (23). As such, the amount of ROS produced in the cells is detected by measuring the fluorescence intensity. Following pseudo-G-Rh2 treatment, A549 cells were collected, washed twice with PBS and incubated with 10 μM DCFH-DA at 37˚C for 20 min in the dark. Cells were subsequently washed three times with PBS. Fluorescence was observed under a Nikon TE-2000U fluorescence microscope (magnification, x100) and measured using flow cytometry as above.

Western blotting. Western blotting was performed to assess protein expression. Following treatment with pseudo-G-Rh2, A549 cells were harvested and lysed in radioimmunoprecipitation assay buffer (Beyotime Biotechnology, Jiangsu, China) for 30 min on ice. The protein concentration was determined using a BCA protein assay kit according to the manufacturer's protocol. Proteins (20 μl) were separated by 12% SDS-PAGE and transferred onto a polyvinylidene fluoride membrane, which was subsequently blocked with 5% (w/v) non-fat milk for 1 h at room temperature. Membranes were incubated with the appropriate primary antibodies against procaspase-3, procaspase-9, PARP, Bcl-2, Bax, Ras, p-Raf, Raf, p53, ERK, c-JNK, p38, p-ERK, p-JNK, p-p38 and β-actin at 1:1,000 dilution at 4˚C overnight. Primary antibody binding was detected by incubation with a secondary antibody conjugated to horseradish peroxidase. The goat-anti-mouse (cat. no. IH-0031) and goat-anti-rabbit (cat. no. IH-0011) secondary antibodies (Beijing Dingguo Changsheng Biotechnology Co., Ltd., Beijing, China) were used at 1:5,000 dilution at room temperature for 1 h. The bands were visualized using a BeyoECL Plus enhanced chemiluminescence kit (Beyotime Institute of Biotechnology). ImageJ software (version 1.5.0.26; National Institutes of Health, Bethesda, MD, USA) was used for analysis.

Statistical analysis. The results are expressed as the mean + standard deviation of three independent experiments. Statistical differences were evaluated using one-way analysis of variance with Tukey's post hoc test. P<0.05 was considered to indicated a statistically significant difference.

Results

Pseudo-G-Rh2 inhibits A549 cell proliferation. To evaluate the antiproliferative effects of pseudo-G-Rh2 *in vitro*, A549 cells were treated with 40, 56, 72, 88 or 140 μM pseudo-G-Rh2 for 24, 48 or 72 h, following which cell viability was assessed by MTT assay. The highest dose of pseudo-G-Rh2 selected was 104 μM, as this is the maximum solubility of this compound in DMSO. The results demonstrated that pseudo-G-Rh2 significantly decreased the viability of A549 cells in a concentration-dependent manner compared with the control (Fig. 2). The IC50 value was 74.5 μM for 24 h. Based on these results, dosages of 24, 48 and 96 μM pseudo-G-Rh2 were selected for further experiments

Pseudo-G-Rh2 induces mitochondria-associated apoptosis in A549 cells. To elucidate whether pseudo-G-Rh2 induces apoptosis, DAPI staining was performed. DAPI staining revealed an increase in the number of apoptotic bodies containing nuclear fragmentations in cells treated with pseudo-G-Rh2 compared with the control group (Fig. 3A and B), which indicates that pseudo-G-Rh2 induces apoptosis in A549 cells. The apoptotic rate was measured using Annexin V-FITC/PI staining and the percentage of apoptotic cells was revealed to be 2.65, 4.44, 14.1 and 48.56% in A549 cells treated with 0, 24, 48 and 96 μM of pseudo-G-Rh2, respectively (Fig. 3C and D). To further investigate the mechanism by which pseudo-G-Rh2 induces apoptosis in A549 cells, the $\Delta\Psi m$ was examined using Rhodamine 123 (Fig. 4A). The $\Delta\Psi m$ (percentage of strong fluorescent cells) in A549 cells treated with 0, 15, 30 and 60 μg/ml pseudo-G-Rh2 for 24 h was 91.35, 88.85, 87.18 and 74.28%, respectively (Fig. 4A and B). In addition, western blotting revealed that the expression of B-cell lymphoma 2 (Bcl-2) was decreased compared with the control, whereas that of Bcl-2-associated X protein (Bax) was increased (Fig. 4C-E). Western blotting revealed that precursors of caspase-9 and caspase-3 were decreased in A549 cells following treatment with pseudo-G-Rh2 treatment compared with the control (Fig. 5A-D). Upregulated cleaved poly ADP-ribose polymerase (PARP), a product of caspase-3, was observed following pseudo-G-Rh2 treatment compared with

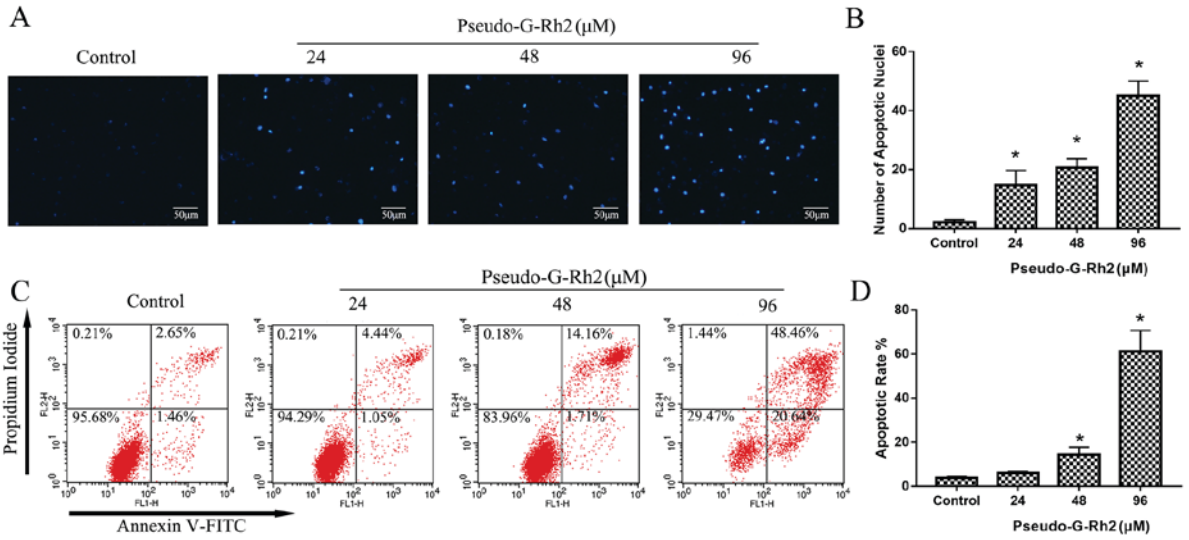

Figure 3. Effect of pseudo-G-Rh2 on apoptosis. (A) Representative photomicrographs and (B) quantified results of DAPI staining in the control and 24, 48 and 96 μM pseudo-G-Rh2 treatment groups. A549 cells were stained with Annexin V-FITC/PI, (C) analyzed by flow cytometry and (D) quantified. Scale bar=50 μm. *P<0.05 vs. control. G, ginsenoside; FITC, fluorescein isothiocyanate; PI, propidium iodide.

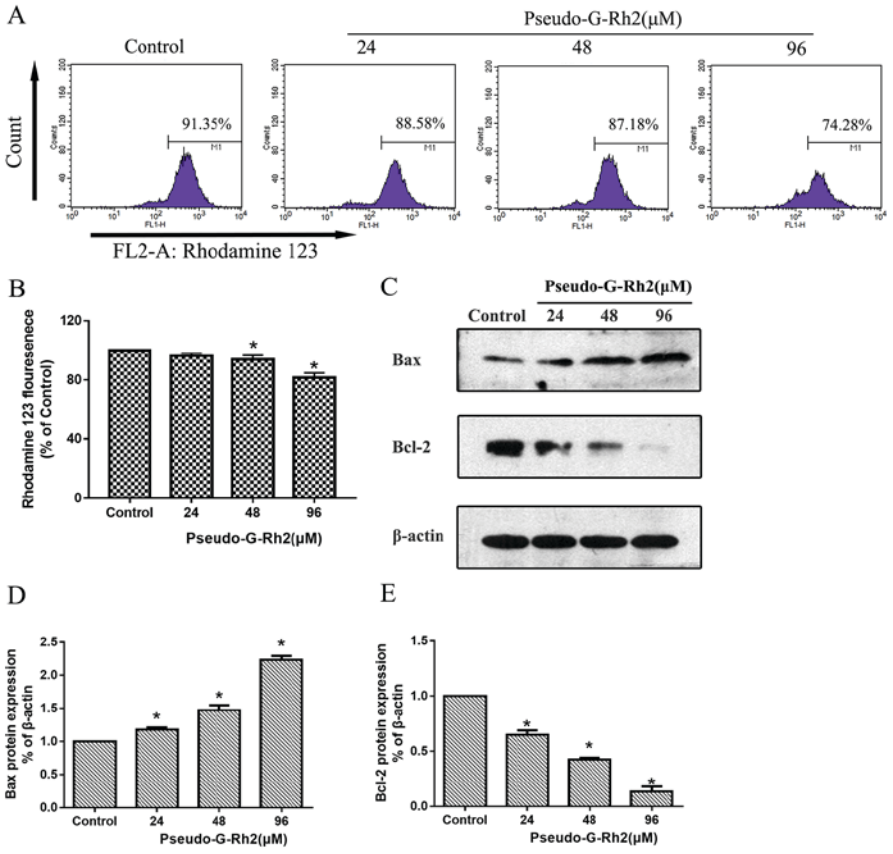

Figure 4. Effect of Pseudo-G-Rh2 on mitochondrial pathways. A549 cells were incubated with 24, 48 or 96 μM pseudo-G-Rh2 for 24 h and Rhodamine 123 dye for 30 min. Fluorescence emission was (A) measured using flow cytometry and (B) quantified. (C) Western blotting was performed and the expression of (D) Bax and (E) Bcl-2 was quantified. *P<0.05 vs. control. G, ginsenoside; Bcl-2, B-cell lymphoma 2; Bax, Bcl-2-associated X protein.

the control. Furthermore, spectrophotometry results revealed that pseudo-G-Rh2 enhanced the activity of caspase-9 and caspase-3 compared with the control (Fig. 5E). These results suggest that pseudo-G-Rh2 induces apoptosis via the mitochondrial pathway in A549 cells.

Pseudo-G-Rh2 increases ROS production. It has previously been reported that ROS serve important roles in mediating cancer initiation, promotion and apoptosis (24,25). To determine whether pseudo-G-Rh2 affects ROS production, A549 cells were treated with 24, 48 or 96 μM pseudo-G-Rh2 for

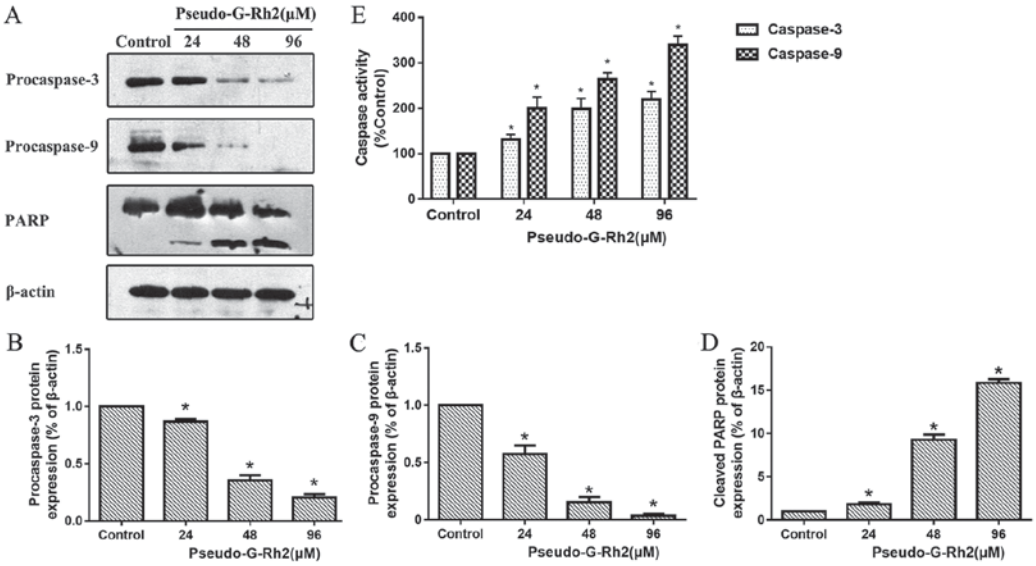

Figure 5. Effects of pseudo-G-Rh2 on caspase activity in A549 cells. A549 cells were incubated with 24, 48 or 96 μM pseudo-G-Rh2 for 24 h. (A) The expression of caspases-9, caspase-3 and PARP was determined using western blotting. (B) Caspase-9 and caspase-3 activities were assessed using Ac-LEHD-pNA and Ac-DEVD-pNA, respectively. Western blotting results for (C) procaspase-3, (D) procaspase-9 and (E) cleaved PARP were quantified. *P<0.05 vs. control. G, ginsenoside; PARP, poly ADP-ribose polymerase.

24 h and subjected to DCFH-DA fluorescence analysis. Pseudo-G-Rh2 increased the intensity of green fluorescence, which indicates ROS-positive cells, in a dose dependent manner compared with the control (Fig. 6A). The results of flow cytometry revealed that ROS expression (percentage of strong fluorescent cells) was 5.84, 7.86, 11.61 and 35.68% in cells treated with 0, 24, 48 or 96 μM pseudo-G-Rh2 for 24 h, respectively (Fig. 6B). These results indicate that pseudo-G-Rh2 induces ROS production in A549 cells, which may lead to apoptosis.

Pseudo-G-Rh2 induces apoptosis via the Ras/Raf/ERK/p53 pathway. ROS is known to be a mediator of mitogen-activated protein kinases (MAPKs) and a number of studies have demonstrated that ROS is able to maintain the activation of Ras, Raf and ERK, resulting in apoptosis and autophagy (9,26,27). In the present study, the expression of Ras, p-Raf and Raf proteins were assessed using western blotting (Fig. 7A). Pseudo-G-Rh2 increased the expression of p-Raf (Fig. 7B), Ras (Fig. 7C) and p53 (Fig. 7D) compared with the control in a dose-dependent manner; meanwhile, the ratio of p-Raf and p-ERK was significantly increased. The expression of MAPK family proteins was also assessed (Fig. 7E) and the results demonstrated that p-ERK (Fig. 7F) was upregulated by pseudo-G-Rh2 in a dose-dependent manner compared with the control. However, pseudo-G-Rh2 had no significant effect on the ratio of p-p38/p38 or p-JNK/JNK. Increased activation of the Ras/Raf/ERK pathway signaling is able to enhance the stability and activity of tumor suppressor p53, which is known to serve an important role in mediating apoptosis (11,28).

Discussion

Pseudo-G-Rh2, a novel derivative of G-Rh2, has previously been demonstrated to have antitumor activity in human gastric cancer SGC-7901 cells (18). In the present study, it was revealed that pseudo-G-Rh2 significantly suppresses cell growth and induces apoptosis in A549 cells *in vitro*. MTT results demonstrated that pseudo-G-Rh2 is cytotoxic in A549 cells, with an IC50 of 74.5 μM. The IC50 obtained in the present study is lower than that reported for SGC-7901 human gastric cancer cells, suggesting that A549 cells are more sensitive to pseudo-G-Rh2 compared with SGC-7901 cells (18). DAPI staining revealed an increase in apoptotic bodies containing nuclear fragments following treatment with pseudo-G-Rh2. An Annexin V-FITC/PI double-staining assay further verified the results of DAPI staining, as the apoptosis percentage increased. Together, these results indicate that pseudo-G-Rh2 exerts its anticancer activity via inducing apoptosis.

Apoptosis comprises a series of complicated and sequential cascade reactions (29). Apoptosis occurs via three pathways: The cell death receptor-mediated extrinsic pathway, the endoplasmic reticulum stress signaling pathway and the mitochondria-mediated intrinsic pathway (30). In the present study, a $\Delta\Psi m$ assay revealed that treatment with pseudo-G-Rh2 decreased the $\Delta\Psi m$ of A549 cells compared with the control. The loss of $\Delta\Psi m$ may result in an increase in mitochondrial cytochrome C release, which in turn promotes activation of the caspase-9 precursor, ultimately leading to apoptosis. Western blotting results revealed that pseudo-G-Rh2 downregulates Bcl-2, procaspase-9 and procaspase-3, whereas Bax and cleaved PARP were upregulated. These results indicate that pseudo-G-Rh2 induces apoptosis in A549 cells via the mitochondrial mediated intrinsic pathway.

The exact mechanisms of pseudo-G-Rh2 are not fully understood. It has been reported that the p38, JNK and ERK pathways, which are the primary pathways of the MAPK family, serve important roles in the proliferation, invasiveness, angiogenesis and cell cycle regulation of a number of cancers, including lung cancer (31,32). The p38 and JNK pathways are

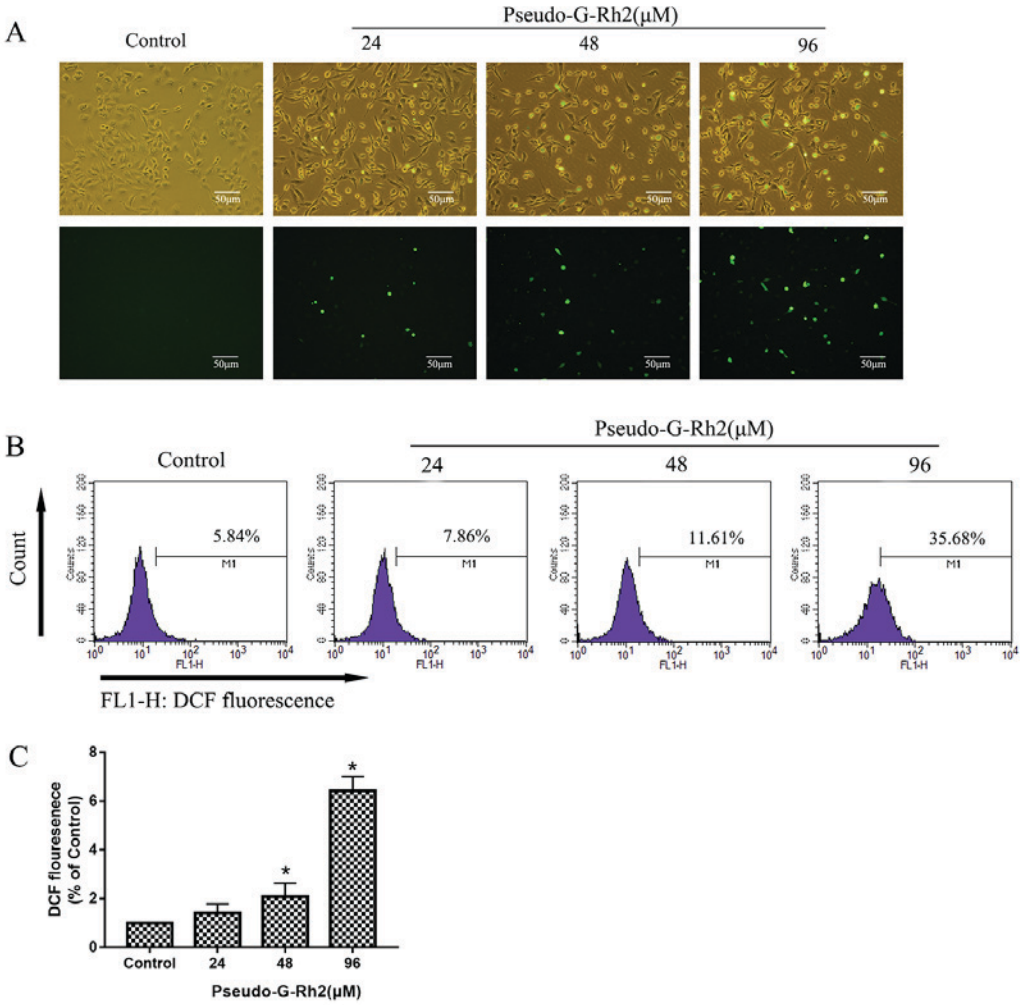

Figure 6. Effect of pseudo-G-Rh2 on ROS. A549 cells were treated with 24, 48 or 96 μM pseudo-G-Rh2 for 24 h. The culture medium was removed and each well was treated with DCF-diacetate solution for 30 min. (A) Fluorescence was observed under an inverted microscope and measured using (B) flow cytometry to assess ROS production. Cells containing a higher amount of ROS emitted hyperfluorescence. (C) Flow cytometry results were subsequently quantified. Scale bar=50 μm *P<0.05, vs. control. G, ginsenoside; ROS, reactive oxygen species; DCF, 2',7'-dichlorofluorescein.

typically associated with cell death and the inhibition of cell proliferation, whereas ERK is associated with cell proliferation (33). However, a number of studies have reported that the ERK pathway may function as tumor suppressor (9,11,34,35). Lv *et al* (11) revealed that Wentilactone A induces apoptosis and G2/M arrest of human lung carcinoma cells via excessive activation of the Ras/Raf/ERK/p53-p21 pathway. Furthermore, Randhawa *et al* (9) reported that the activation of ERK signaling serves a role in the induction of colon cancer apoptosis by piperlongumine. These inconsistencies may be due to variations in the strength of the cascade signal and external stimuli, including ROS (8). During early-stage tumor development, ROS affects gene expression and genome stability, resulting in loss-of-function mutations in p53 (36). Furthermore, ROS induces metabolic adaptations (37), which are crucial for the pathogenesis of cancer. However, during the later stages of cancer, ROS accumulation induces p53 expression, which in turn causes cell cycle arrest at the G2/M phase, DNA fragmentation and apoptosis (38). It has been reported that G may induce cell cycle arrest or cell death by increasing ROS release in cancer cells (39,40). ROS has also been reported to be a mediator of ERK-induced cell death (41,42); specifically, elevated ROS results in sustained ERK activity, which in turn causes enhanced p53 expression (43). p53 protein is associated with Bcl-2 family regulation and is believed to serve a critical role in mediating apoptosis (43,44). ERK activity has been reported to directly affect mitochondrial function by decreasing mitochondrial respiration and $\Delta\Psi m$, which may lead to mitochondrial membrane disruption and cytochrome c release (45,46). In addition, Ras/Raf/ERK activity has been reported to be associated with the upregulation of proapoptotic members of the Bcl-2 family, including Bax and p53 upregulated modulator of apoptosis, as well as the downregulation of Bcl-2 and Bcl-extra large (44,47,48).

In the present study, the effect of pseudo-G-Rh2 on the Ras/Raf/ERK pathway was assessed by measuring the expression of total Ras/Raf/ERK and p-Ras/Raf/ERK family members. The results demonstrated that pseudo-G-Rh2 significantly increased the ratio of p-Raf and p-ERK in A549 cells *in vitro*, whereas no significant changes were observed in the ratio of p-p38/p38 and p-JNK/JNK. These results suggest that pseudo-G-Rh2 induces apoptosis in A549 cells via the Ras/Raf/ERK pathway, which was further confirmed by the increase in ROS levels and upregulation of p53.

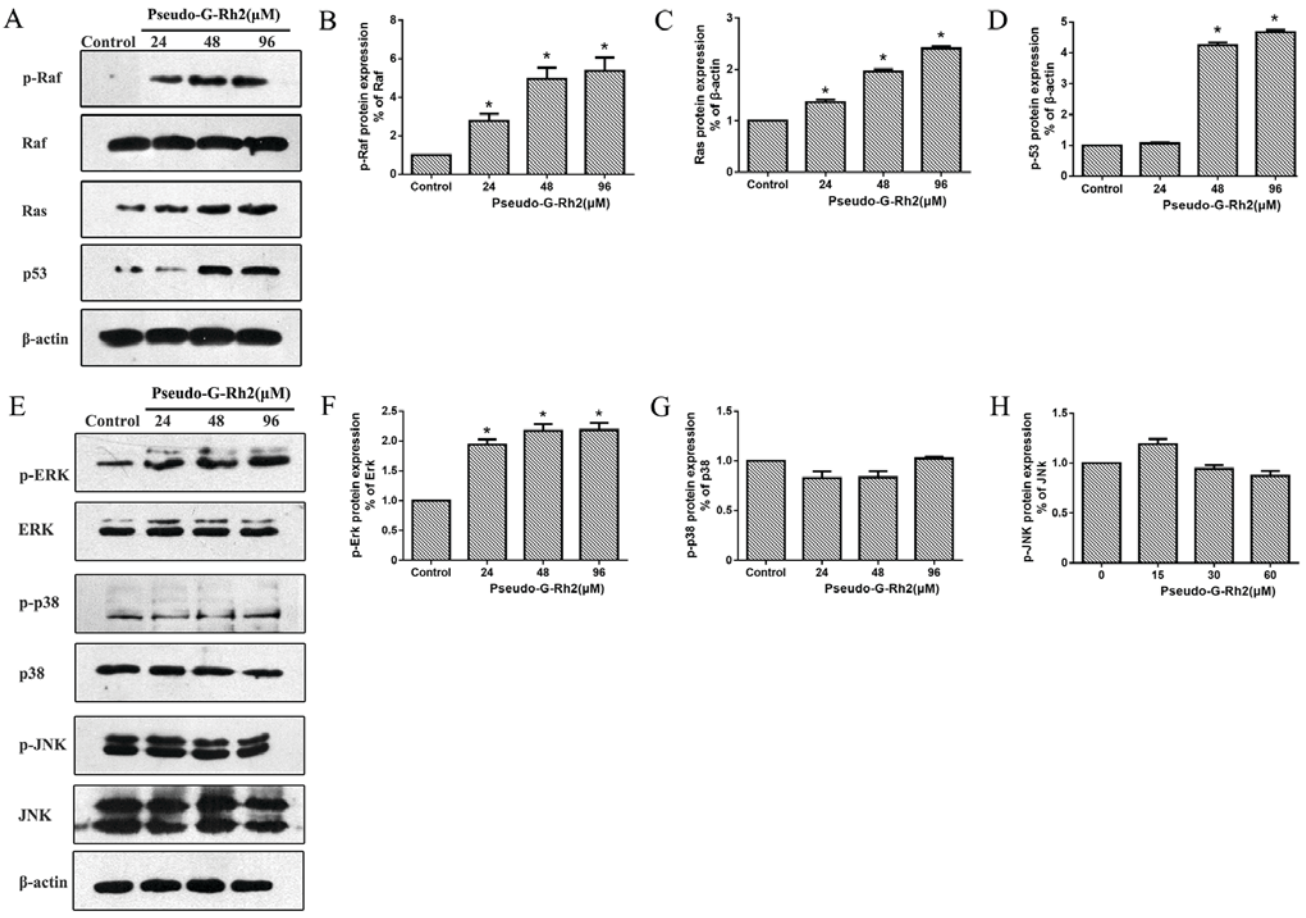

Figure 7. Effect of pseudo-G-Rh2 on the Ras/Raf, p53 and MAPK pathway. (A) A549 cells were incubated with 24, 48 or 96 μM pseudo-G-Rh2 for 24 h and assessed using western blotting. The expression of (B) p-Raf, (C) Ras and (D) p53 was quantified. (E) Western blotting was also performed to assess the expression of MAPK members (F) p-ERK, (G) p-p38 and (H) p-JNK. *P<0.05 vs. control. G, ginsenoside; MAPK, mitogen activated protein kinase; p, phosphorylated; ERK, extracellular signal-regulated kinase; JNK, c-Jun N-terminal kinase.

In conclusion, the results of the present study demonstrated that pseudo-G-Rh2 induced apoptosis in lung adenocarcinoma A549 cells via the mitochondrial mediated intrinsic pathway. During this process, pseudo-G-Rh2 increased ROS generation and caused the subsequent activation of the Ras/Raf/ERK/p53 signaling pathway. These results provide an insight into the mechanism of pseudo-G-Rh2-induced adenocarcinoma cell apoptosis, suggesting that pseudo-G-Rh2 may have potential as a chemotherapeutic agent for the treatment of lung adenocarcinoma. However, the present study is with limitations. It was confirmed that the activation of the Ras/Raf/ERK/p53 signaling pathway was involved in the apoptosis induced by pseudo-G-Rh2, however whether the Ras/Raf/ERK/p53 signaling pathway is the only target of pseudo-G-Rh2 remains unclear. Further investigation is required to confirm the mechanisms of pseudo-G-Rh2 by employing specific inhibitors of the Ras-ERK signaling pathway. In addition, the authors intend to utilize multi time point treatments of pseudo-G-Rh2 and other lung cancer cell lines in the future to confirm the effect of pseudo-G-Rh2 in NSCLC.

Acknowledgements

The authors would like to thank Dr Huiping Du, Department of Health Informatics, Georgia State University (Atlanta, GA, USA), for her critical reading and language editing.

Funding

This study was supported by Jilin Province Department of Education (grant no. JLE20130105).

Availability of data and materials

The datasets used and/or analyzed during the current study are available from the corresponding author on reasonable request.

Authors' contributions

DS and HX conceived and designed the study. CL, YT, XY, YW and ZL performed the experiments. YW and HX wrote the paper. CL, YT, XY and YW reviewed and edited the manuscript. All authors read and approved the final manuscript.

Ethics approval and consent to participate

Not applicable

Consent for publication

Not applicable

Competing interests

The authors declare that they have no competing interests.

References

1. Chen W, Zheng R, Zeng H and Zhang S: Epidemiology of lung cancer in China. Thorac Cancer 6: 209-215, 2015.
2. Burstein HJ and Schwartz RS: Molecular origins of cancer. N Engl J Med 358: 527, 2008.
3. Uramoto H and Tanaka F: Recurrence after surgery in patients with NSCLC. Transl Lung Cancer Res 3: 242-249, 2014.
4. Rittmeyer A: Quality of life in patients with NSCLC receiving maintenance therapy. Cancers (Basel) 7: 950-962, 2015.
5. Leidinger P, Brefort T, Backes C, Krapp M, Galata V, Beier M, Kohlhaas J, Huwer H, Meese E and Keller A: High-throughput qRT-PCR validation of blood microRNAs in non-small cell lung cancer. Oncotarget 7: 4611-4623, 2016.
6. Balmanno K and Cook SJ: Tumour cell survival signalling by the ERK1/2 pathway. Cell Death Differ 16: 368-377, 2009.
7. Cox AD and Der CJ: The dark side of Ras: Regulation of apoptosis. Oncogene 22: 8999-9006, 2003.
8. Cagnol S and Chambard JC: ERK and cell death: Mechanisms of ERK-induced cell death-apoptosis, autophagy and senescence. FEBS J 277: 2-21, 2010.
9. Randhawa H, Kibble K, Zeng H, Moyer MP and Reindl KM: Activation of ERK signaling and induction of colon cancer cell death by piperlongumine. Toxicol In Vitro 27: 1626-1633, 2013.
10. Bacus SS, Gudkov AV, Lowe M, Lyass L, Yung Y, Komarov AP, Keyomarsi K, Yarden Y and Seger R: Taxol-induced apoptosis depends on MAP kinase pathways (ERK and p38) and is independent of p53. Oncogene 20: 147-155, 2001.
11. Lv C, Hong Y, Miao L, Li C, Xu G, Wei S, Wang B, Huang C and Jiao B: Wentilactone A as a novel potential antitumor agent induces apoptosis and G2/M arrest of human lung carcinoma cells, and is mediated by HRas-GTP accumulation to excessively activate the Ras/Raf/ERK/p53-p21 pathway. Cell Death Dis 4: e952, 2013.
12. Liu T, Zhao L, Zhang Y, Chen W, Liu D, Hou H, Ding L and Li X: Ginsenoside 20(S)-Rg3 targets HIF-1α to block hypoxia-induced epithelial-mesenchymal transition in ovarian cancer cells. PLoS One 9: e103887, 2014.
13. Kiefer D and Pantuso T: Panax ginseng. Am Fam Physician 68: 1539-1542, 2003.
14. Zhang C, Yu H and Hou J: Effects of 20 (S)-ginsenoside Rh2 and 20 (R)-ginsenoside Rh2 on proliferation and apoptosis of human lung adenocarcinoma A549 cells. Zhongguo Zhong Yao Za Zhi 36: 1670-1674, 2011 (In Chinese).
15. Oh M, Choi YH, Choi S, Chung H, Kim K, Kim SI, Kim DK and Kim ND: Anti-proliferating effects of ginsenoside Rh2 on MCF-7 human breast cancer cells. Int J Oncol 14: 869-875, 1999.
16. Liu YF, Yuan HN, Bi XL, Piao HR, Cao JQ, Li W, Wang P and Zhao YQ: 25-Methoxylprotopanaxadiol derivatives and their anti-proliferative activities. Steroids 78: 1305-1311, 2013.
17. Qian G, Wang Z, Zhao J, Li D, Gao W, Wang B, Sui D, Qu X and Chen Y: Synthesis and anti-cancer cell activity of pseudo-ginsenoside Rh2. Steroids 92: 1-6, 2014.
18. Qu X, Qu S, Yu X, Xu H, Chen Y, Ma X and Sui D: Pseudo-G-Rh2 induces mitochondrial-mediated apoptosis in SGC-7901 human gastric cancer cells. Oncol Rep 26: 1441-1446, 2011.
19. Xu HL, Yu XF, Qu SC, Zhang R, Qu XR, Chen YP, Ma XY and Sui DY: Anti-proliferative effect of Juglone from Juglans mandshurica Maxim on human leukemia cell HL-60 by inducing apoptosis through the mitochondria-dependent pathway. Eur J Pharmacol 645: 14-22, 2010.
20. Matin MM, Nakhaeizadeh H, Bahrami AR, Iranshahi M, Arghiani N and Rassouli FB: Ferutinin, an apoptosis inducing terpenoid from Ferula ovina. Asian Pac J Cancer Prev 15: 2123-2128, 2014.
21. Chen HY, Zhang X, Chen SF, Zhang YX, Liu YH, Ma LL and Wang LX: The protective effect of 17β-estradiol against hydrogen peroxide-induced apoptosis on mesenchymal stem cell. Biomed Pharmacother 66: 57-63, 2012.
22. Deeb D, Gao X, Jiang H, Janic B, Arbab AS, Rojanasakul Y, Dulchavsky SA and Gautam SC: Oleanane triterpenoid CDDO-Me inhibits growth and induces apoptosis in prostate cancer cells through a ROS-dependent mechanism. Biochem Pharmacol 79: 350-360, 2010.
23. Wang H and Joseph JA: Quantifying cellular oxidative stress by dichlorofluorescein assay using microplate reader. Free Radic Biol Med 27: 612-616, 1999.
24. Feng X, Yu W, Zhou F, Chen J and Shen P: A novel small molecule compound diaporine inhibits breast cancer cell proliferation via promoting ROS generation. Biomed Pharmacother 83: 1038-1047, 2016.
25. Trachootham D, Alexandre J and Huang P: Targeting cancer cells by ROS-mediated mechanisms: A radical therapeutic approach? Nat Rev Drug Discov 8: 579-591, 2009.
26. Lee YJ, Cho HN, Soh JW, Jhon GJ, Cho CK, Chung HY, Bae S, Lee SJ and Lee YS: Oxidative stress-induced apoptosis is mediated by ERK1/2 phosphorylation. Exp Cell Res 291: 251-266, 2003.
27. Zhang P, Wang YZ, Kagan E and Bonner JC: Peroxynitrite targets the epidermal growth factor receptor, Raf-1, and MEK independently to activate MAPK. J Biol Chem 275: 22479-22486, 2000.
28. Ringer L, Sirajuddin P, Tricoli L, Waye S, Choudhry MU, Parasido E, Sivakumar A, Heckler M, Naeem A, Abdelgawad I, *et al*: The induction of the p53 tumor suppressor protein bridges the apoptotic and autophagic signaling pathways to regulate cell death in prostate cancer cells. Oncotarget 5: 10678-10691, 2014.
29. Tsuruo T, Naito M, Tomida A, Fujita N, Mashima T, Sakamoto H and Haga N: Molecular targeting therapy of cancer: Drug resistance, apoptosis and survival signal. Cancer Sci 94: 15-21, 2003.
30. Abraham MC and Shaham S: Death without caspases, caspases without death. Trends Cell Biol 14: 184-193, 2004.
31. Shi C, Zheng DD, Fang L, Wu F, Kwong WH and Xu J: Ginsenoside Rg1 promotes nonamyloidgenic cleavage of APP via estrogen receptor signaling to MAPK/ERK and PI3K/Akt. Biochim Biophys Acta 1820: 453-460, 2012.
32. Choi YJ, Yoon JH, Cha SW and Lee SG: Ginsenoside Rh1 inhibits the invasion and migration of THP-1 acute monocytic leukemia cells via inactivation of the MAPK signaling pathway. Fitoterapia 82: 911-919, 2011.
33. Zhang C, Zhu H, Yang X, Lou J, Zhu D, Lu W, He Q and Yang B: P53 and p38 MAPK pathways are involved in MONCPT-induced cell cycle G2/M arrest in human non-small cell lung cancer A549. J Cancer Res Clin Oncol 136: 437-445, 2010.
34. Shih A, Davis FB, Lin HY and Davis PJ: Resveratrol induces apoptosis in thyroid cancer cell lines via a MAPK- and p53-dependent mechanism. J Clin Endocrinol Metab 87: 1223-1232, 2002.
35. Wang X, Martindale JL and Holbrook NJ: Requirement for ERK activation in cisplatin-induced apoptosis. J Biol Chem 275: 39435-39443, 2000.
36. Waris G and Ahsan H: Reactive oxygen species: Role in the development of cancer and various chronic conditions. J Carcinog 5: 14, 2006.
37. Weinberg F, Hamanaka R, Wheaton WW, Weinberg S, Joseph J, Lopez M, Kalyanaraman B, Mutlu GM, Budinger GR and Chandel NS: Mitochondrial metabolism and ROS generation are essential for Kras-mediated tumorigenicity. Proc Natl Acad Sci USA 107: 8788-8793, 2010.
38. Wu CL, Huang AC, Yang JS, Liao CL, Lu HF, Chou ST, Ma CY, Hsia TC, Ko YC and Chung JG: Benzyl isothiocyanate (BITC) and phenethyl isothiocyanate (PEITC)-mediated generation of reactive oxygen species causes cell cycle arrest and induces apoptosis via activation of caspase-3, mitochondria dysfunction and nitric oxide (NO) in human osteogenic sarcoma U-2 OS cells. J Orthop Res 29: 1199-1209, 2011.
39. Ge G, Yan Y and Cai H: Ginsenoside Rh2 inhibited proliferation by inducing ROS mediated ER stress dependent apoptosis in lung cancer cells. Biol Pharm Bull 40: 2117-2124, 2017.
40. Singh DV, Agarwal S, Singh P, Godbole MM and Misra K: Curcumin conjugates induce apoptosis via a mitochondrion dependent pathway in MCF-7 and MDA-MB-231 cell lines. Asian Pac J Cancer Prev 14: 5797-5804, 2013.
41. Matsunaga Y, Kawai Y, Kohda Y and Gemba M: Involvement of activation of NADPH oxidase and extracellular signal-regulated kinase (ERK) in renal cell injury induced by zinc. J Toxicol Sci 30: 135-144, 2005.
42. Ramachandiran S, Huang Q, Dong J, Lau SS and Monks TJ: Mitogen-activated protein kinases contribute to reactive oxygen species-induced cell death in renal proximal tubule epithelial cells. Chem Res Toxicol 15: 1635-1642, 2002.

43. Woessmann W, Chen X and Borkhardt A: Ras-mediated activation of ERK by cisplatin induces cell death independently of p53 in osteosarcoma and neuroblastoma cell lines. Cancer Chemother Pharmacol 50: 397-404, 2002.
44. DeHaan RD, Yazlovitskaya EM and Persons DL: Regulation of p53 target gene expression by cisplatin-induced extracellular signal-regulated kinase. Cancer Chemother Pharmacol 48: 383-388, 2001.
45. Kim GS, Hong JS, Kim SW, Koh JM, An CS, Choi JY and Cheng SL: Leptin induces apoptosis via ERK/cPLA2/cytochrome c pathway in human bone marrow stromal cells. J Biol Chem 278: 21920-21929, 2003.
46. Li DW, Liu JP, Mao YW, Xiang H, Wang J, Ma WY, Dong Z, Pike HM, Brown RE and Reed JC: Calcium-activated RAF/MEK/ERK signaling pathway mediates p53-dependent apoptosis and is abrogated by alpha B-crystallin through inhibition of RAS activation. Mol Biol Cell 16: 4437-4453, 2005.
47. Liu J, Mao W, Ding B and Liang CS: ERKs/p53 signal transduction pathway is involved in doxorubicin-induced apoptosis in H9c2 cells and cardiomyocytes. Am J Physiol Heart Circ Physiol 295: H1956-H1965, 2008.
48. Wu Z, Wu LJ, Tashiro S, Onodera S and Ikejima T: Phosphorylated extracellular signal-regulated kinase up-regulated p53 expression in shikonin-induced HeLa cell apoptosis. Chin Med J (Engl) 118: 671-677, 2005.